Vertical sorting and the morphodynamics of bed form–dominated rivers: A modeling framework

Astrid Blom
Water Engineering and Management, Civil Engineering, University of Twente, Enschede, The Netherlands

Gary Parker
St. Anthony Falls Laboratory, University of Minnesota, Minneapolis, Minnesota, USA

Received 29 July 2003; revised 23 February 2004; accepted 14 April 2004; published 10 June 2004.

[1] Uncertainties and errors in predictions by morphodynamic models of rivers with nonuniform sediment are usually attributed to shortcomings pertaining to the submodel of sediment transport. This mistakenly neglects shortcomings in the submodel of sediment continuity, which describes the vertical sorting and the bed surface composition, whereas the latter is one of the main input parameters for calculating sediment transport and thus morphological changes. *Hirano* [1971, 1972] was the first to develop a sediment continuity model for nonuniform sediment. Since this commonly used Hirano active layer model and its variants suffer from a number of shortcomings, the authors have developed a new type of sediment continuity model that describes the bed composition and vertical sorting fluxes without distinguishing discrete bed layers. This continuum sorting model is aimed at conditions dominated by bed forms and bed load transport. It is based on (1) the Parker-Paola-Leclair framework for sediment continuity, (2) the Einstein step length formulation, (3) a newly developed lee sorting function, and (4) a newly developed method to account for the variability in bed form trough elevations. The resulting model is deterministic in the computation of the vertical sorting profile and is probabilistic in terms of the riverbed surface due to the presence of dunes. *INDEX TERMS:* 1815 Hydrology: Erosion and sedimentation; 1824 Hydrology: Geomorphology (1625); 1869 Hydrology: Stochastic processes; 3210 Mathematical Geophysics: Modeling; *KEYWORDS:* river morphodynamics, sediment sorting, sediment mixtures, bed forms, modeling

Citation: Blom, A., and G. Parker (2004), Vertical sorting and the morphodynamics of bed form–dominated rivers: A modeling framework, *J. Geophys. Res.*, *109*, F02007, doi:10.1029/2003JF000069.

1. Introduction

[2] In morphological river models the bed material may be characterized by one specific grain size in cases where sediment sorting processes do not play a role. Vertical, lateral, or longitudinal sorting of the bed material may occur when the river bed is characterized by a range in grain sizes as fine grains are picked up and transported more easily than coarse ones. Through affecting the small-scale morphology (e.g., dune dimensions, bed surface composition, and bed roughness), sediment sorting also influences grain size-selective sediment transport, changes in mean bed level, and water levels.

[3] A change in mean bed level results from divergences in the transport rate, which is expressed by the sediment continuity equation or mass balance equation. In cases where the bed material consists of multiple size fractions, divergences in the transport rate of size fractions will result in a change in the composition of the bed surface and/or aggradation or degradation of the river bed. A further complication in the mass balance is the preference of certain size fractions to be deposited at specific bed elevations, i.e., the vertical sorting. A plane bed is often covered with a coarse bed layer (mobile pavement or armor layer), whereas under bed form conditions the coarse size fractions are mainly found in the lower parts of the bed forms (Figure 1).

[4] *Blom et al.* [2003] describe sediment sorting mechanisms that play a role under bed form-dominated conditions. The above mentioned downward coarsening trend of bed form material results from the avalanching of grains down the bed form lee face [*Bagnold*, 1941; *Allen*, 1965]. When conditions are well above the shear stresses for incipient motion of all size fractions in the mixture, the coarse sediment in the lower parts of the bed forms takes part in the sediment transport processes. When conditions of partial transport prevail and a significant amount of coarse material is not or is barely transported by the flow, the coarse sediment gathers below the migrating bed forms, forming an essentially immobile coarse layer. Besides the avalanching process at the bed form lee face and partial transport, the winnowing of fines from the trough surface and subsurface also contributes to the formation of a coarse bed layer underneath migrating bed forms.

0148-0227/04/2003JF000069

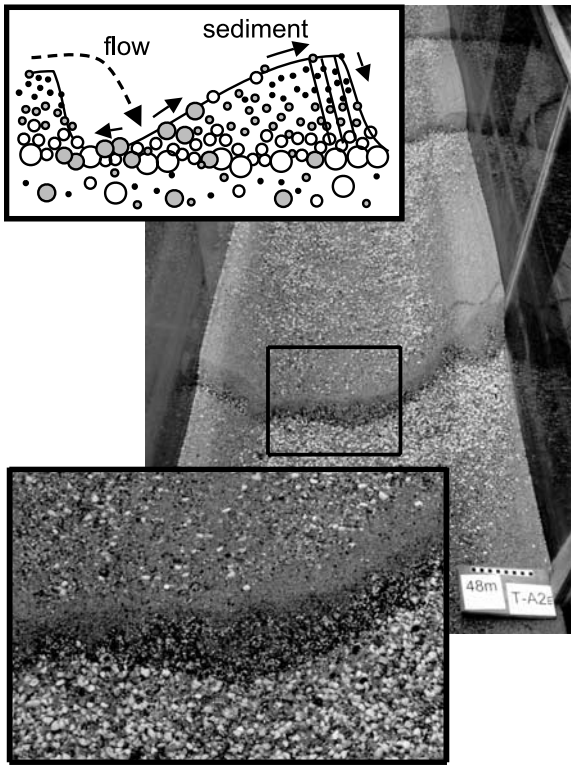

Figure 1. Flume experiment A2E conducted by *Blom et al.* [2003], with an interpretation of the vertical sorting pattern. The flow is from top to bottom.

[5] The interaction among grain size-selective sediment transport, vertical sorting, and net aggradation or degradation is described in terms of sediment continuity models. *Blom* [2003] distinguishes four types of sediment continuity models: burial depth models, bed layer models, grain-scale models, and depth-continuous models. Burial depth models describe the time evolution of the transport of (tracer) particles and their burial into the bed [e.g., *Crickmore and Lean*, 1962]. Strictly speaking, burial depth models are not true sediment continuity models as they do not describe the above interaction. Bed layer models are sediment continuity models in which the bed is divided into a certain number of discrete and homogeneous bed layers [e.g., *Hirano*, 1971]. Grain-scale models are defined as sediment continuity models that consider sediment entrainment and deposition at the scale of grains [e.g., *Tsujimoto and Motohashi*, 1990], whereas the other types consider processes at a scale of a large number of bed forms. Depth-continuous models do not distinguish discrete bed layers [*Armanini*, 1995; *Parker et al.*, 2000]. They include a probability density function of bed surface elevations so as to account for the likelihood of a bed elevation being exposed to the flow.

[6] *Hirano* [1971, 1972] was the first to develop a sediment continuity model for nonuniform sediment. In his active layer model the bed is divided into a homogeneous top layer, i.e., the active layer, and a nonmoving substrate. The active layer represents the part of the bed that interacts with the flow and that determines the rate and composition of the transported sediment. Sediment fluxes between the active layer and the substrate occur in case of net aggradation or degradation only. Various authors have proposed additions to the Hirano active layer model [also see *Blom*, 2003]: (1) introduction of a term describing the time evolution of the storage of sediment in a thin bed load layer on top of the active layer [*Armanini and Di Silvio*, 1988; *Parker*, 1991; *Di Silvio*, 1992]; (2) introduction of a formulation for suspended load transport [*Armanini and Di Silvio*, 1988; *Holly and Rahuel*, 1990; *Di Silvio*, 1992]; (3) introduction of a formulation for particle abrasion [*Parker*, 1991]; (4) modifications to the composition of the depositional flux to the substrate [*Parker*, 1991; *Hoey and Ferguson*, 1994; *Toro-Escobar et al.*, 1996]; (5) introduction of an additional layer below the active layer to account for vertical sediment exchange due to occasionally deep bed form troughs [*Ribberink*, 1987; *Di Silvio*, 1992]; (6) subdivision of the nonmoving substrate into different layers for bookkeeping purposes [*Sloff et al.*, 2001]; and (7) introduction of a mixing coefficient to account for the effects of biological mixing on tidal flats in estuaries (i.e., bioturbation) [*Van Ledden and Wang*, 2001]. Yet, the Hirano bed layer model and its variants suffer from a number of shortcomings. They fail to describe vertical sorting fluxes through bed form migration, i.e., through grain size-selective deposition down the bed form lee face and the variability in trough elevations. In most sediment continuity models, vertical sediment fluxes within the bed occur through net aggradation or degradation only, whereas flume experiments have shown that these fluxes also occur in situations without net aggradation or degradation [e.g., *Blom et al.*, 2003]. Another problem of the bed layer models is that in certain situations, their set of equations becomes elliptic in parts of the space-time domain [*Ribberink*, 1987]. Solving the set of equations then requires future time boundaries, which is physically unrealistic. A final problem is that the definition of the thickness of the bed layers remains rather arbitrary. From a physical point of view, it is not straightforward to distinguish between the range of bed elevations interacting with the flow regularly (i.e., the active layer), the range interacting with the flow only occasionally (i.e., the exchange layer in the Ribberink two-layer model), and the range not interacting with the flow at all (i.e., the substrate). In morphological models the bed layers' thicknesses are therefore usually simply used as calibration parameters.

[7] In order to overcome these shortcomings, the authors have developed a new depth-continuous sediment continuity model, i.e., a continuum sorting model. The present paper describes its components and its derivation. The continuum sorting model is based on the framework for sediment continuity introduced by *Parker et al.* [2000]. This Parker-Paola-Leclair (PPL) framework offers the possibility of describing the vertical sorting fluxes continuously over bed elevations and relating the sorting fluxes at a certain bed elevation to its likelihood of being exposed to the flow. The PPL model is called a framework as formulations for the grain size-specific and elevation-specific entrainment and deposition fluxes remained to be derived. In the present paper the authors derive formulations for these fluxes for conditions dominated by bed forms and bed load transport.

[8] While this paper describes a new mathematical modeling framework for taking into account the impact of vertical sorting upon the large-scale morphodynamics of

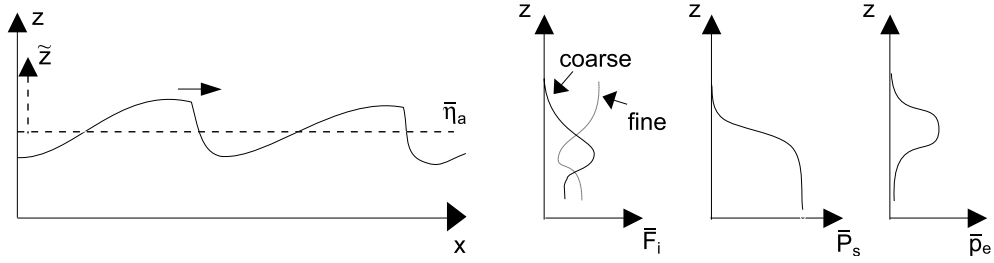

Figure 2. A series of bed forms, for which $\bar{F}_i$ expresses the volume fraction content of size fraction i at elevation z, $\bar{P}_s$ the probability that the bed surface elevation is higher than z, $\bar{p}_e$ is the probability density that the bed surface elevation is equal to z, and $\bar{\eta}_a$ is the mean bed level.

bed form-dominated rivers, two follow-up papers (A. Blom et al., manuscripts in preparation, 2004) will consider the simplification of this modeling framework to two reduced sorting models (an equilibrium sorting model and a sorting evolution model, respectively) as well as application of these reduced models to measured data from flume experiments.

2. Parker-Paola-Leclair (PPL) Framework for Sediment Continuity

[9] Sediment conservation of size fraction i at elevation z is given by *Parker et al.* [2000]:

$$\frac{\partial \bar{C}_i}{\partial t} = c_b \bar{P}_s \frac{\partial \bar{F}_i}{\partial t} + c_b \bar{F}_i \frac{\partial \bar{P}_s}{\partial t} = \bar{D}_{ei} - \bar{E}_{ei}, \tag{1}$$

where $\bar{C}_i(x, z, t)$ denotes the concentration of size fraction i at elevation z ($\bar{C}_i = c_b \bar{P}_s \bar{F}_i$), $\bar{D}_{ei}(x, z, t)$ denotes the deposition density of size fraction i defined such that $\bar{D}_{ei}dxdz$ is the volume of sediment of size fraction i that is deposited per unit width and time in a bed element with sides dx and dz at elevation z, $\bar{E}_{ei}(x, z, t)$ denotes the entrainment density of size fraction i defined likewise, $\bar{F}_i(x, z, t)$ denotes the volume fraction content of size fraction i at elevation z (Figure 2), $\bar{P}_s(x, z, t)$ denotes the probability distribution of bed surface elevations indicating the probability that the bed elevation is higher than z, and c_b denotes the concentration of sediment in the bed ($c_b = 1 - \lambda_b$, where λ_b denotes the porosity). The bar indicates that the parameter is averaged over some horizontal distance, e.g., a large number of bed forms, x denotes the horizontal coordinate on the scale of series of bed forms, z denotes the vertical coordinate, and t denotes the time coordinate.

[10] The probability density function (PDF) of bed surface elevations, $\bar{p}_e(x, z, t)$, expresses the probability density that the bed surface elevation equals z or the likelihood of elevation z being exposed to the flow (Figure 2). Integration of the PDF of bed surface elevations, $\bar{p}_e$, over bed elevations $-\infty$ to z yields the probability of exceeding a certain bed elevation, $\bar{P}_s$:

$$\bar{P}_s = 1 - \int_{-\infty}^{z} \bar{p}_e dz, \tag{2}$$

where $\bar{P}_s$ not only indicates the probability that the bed surface elevation is higher than z but also equals the proportion of the bed at elevation z that is covered with sediment [*Crickmore and Lean*, 1962].

[11] We now perform the following coordinate transformation: $\tilde{x} = x$, $\tilde{t} = t$, and $\tilde{z} = z - \bar{\eta}_a$, wherein $\tilde{z}$ is the deviation from the mean bed level, $\bar{\eta}_a(x, t)$ (Figure 2). Applying the chain rule yields that the time derivative $\partial \bar{P}_s/\partial t$ in equation (1) can be written as

$$\frac{\partial \bar{P}_s}{\partial t} = \frac{\partial \tilde{P}_s}{\partial t} - \frac{\partial \tilde{P}_s}{\partial \tilde{z}} \frac{\partial \bar{\eta}_a}{\partial t} = \frac{\partial \tilde{P}_s}{\partial t} + \bar{p}_e \frac{\partial \bar{\eta}_a}{\partial t} \tag{3}$$

since

$$\bar{p}_e = -\frac{\partial \bar{P}_s}{\partial z} = -\frac{\partial \tilde{P}_s}{\partial \tilde{z}}, \tag{4}$$

where $\tilde{P}_s(\tilde{x}, \tilde{z}, \tilde{t})$ denotes the probability distribution of bed surface elevations relative to the mean bed level, $\bar{\eta}_a$. With equation (3), equation (1) becomes

$$c_b \bar{P}_s \frac{\partial \bar{F}_i}{\partial t} + c_b \bar{F}_i \frac{\partial \tilde{P}_s}{\partial t} + c_b \bar{F}_i \bar{p}_e \frac{\partial \bar{\eta}_a}{\partial t} = \bar{D}_{ei} - \bar{E}_{ei}. \tag{5}$$

Adding up equation (5) over all grain sizes yields

$$c_b \frac{\partial \tilde{P}_s}{\partial t} + c_b \bar{p}_e \frac{\partial \bar{\eta}_a}{\partial t} = \bar{D}_e - \bar{E}_e, \tag{6}$$

where $\bar{D}_e(x, z, t)$ denotes the deposition density defined such that $\bar{D}_e dxdz$ is the volume of all size fractions deposited in a bed element with sides dx and dz at elevation z per unit width and time ($\bar{D}_e = \sum_i^N \bar{D}_{ei}$, where N denotes the total number of size fractions) and $\bar{E}_e(x, z, t)$ the entrainment density defined likewise ($\bar{E}_e = \sum_i^N \bar{E}_{ei}$). Integration of equation (6) over all bed elevations yields

$$c_b \int_{-\infty}^{\infty} \frac{\partial \tilde{P}_s}{\partial t} dz + c_b \frac{\partial \bar{\eta}_a}{\partial t} = \bar{D} - \bar{E}, \tag{7}$$

where $\bar{D}(x, t)$ denotes the volume of all grain sizes deposited per unit area and time ($\bar{D} = \int_{-\infty}^{\infty} \bar{D}_e dz$) and $\bar{E}(x, t)$ denotes the volume of all grain sizes entrained per unit area and time ($\bar{E} = \int_{-\infty}^{\infty} \bar{E}_e dz$). Appendix A shows that the integral in equation (7) equals zero so that equation (7) reduces to

$$c_b \frac{\partial \bar{\eta}_a}{\partial t} = \bar{D} - \bar{E} \left(= -\frac{\partial \bar{q}_a}{\partial x} \right), \tag{8}$$

in which we recognize the sediment continuity or mass balance equation, where $\bar{q}_a(x, t)$ denotes the bed load transport rate averaged over a series of bed forms.

[12] Equations (5), (6), and (8) compose the fundamental set of equations of the PPL framework for sediment continuity. Now, to complete this set of equations, we will derive formulations for the deposition and entrainment densities, $\bar{D}_{ei}$ and $\bar{E}_{ei}$, for bed form-dominated conditions. This is done in a few steps. First, we will analyze the migration of a single bed form, in which we successively derive a relation between the grain size-specific deposition and entrainment fluxes over the bed form stoss face (section 3.1), derive a formulation for the deposition rate over the lee face (section 3.2), derive a formulation for the composition of the lee deposit (section 3.3), convert the equations into bed elevation-specific ones (section 3.4), and develop a model describing the grain size-specific deposition down the lee face of a single bed form (section 3.5). Secondly, we will couple the single bed form migration approach to the PPL framework (section 4.1). Then, we will introduce the irregularity of bed forms by incorporating the statistics of bed form trough elevations (section 4.2). Section 5 will briefly describe the reduction of the resulting continuum sorting model to both an equilibrium sorting model and a sorting evolution model, which will be explained in detail in two follow-up papers (A. Blom et al., manuscripts in preparation, 2004). Section 6 presents some results of two submodels of the continuum sorting model.

3. Migration of a Single Bed Form

3.1. Einstein Step Length Formulation

[13] We now divide each bed form into a stoss and a lee face (Figure 3) and assume that on the stoss side, deposition and entrainment occur simultaneously, while on the lee side, only deposition occurs. At the stoss face we apply the step length formulation first introduced by *Einstein* [1950] in order to relate the grain size-specific deposition rate over the bed form stoss face to the grain size-specific entrainment rate. The Einstein step length, Λ, is defined as the average distance covered by a particle from the moment it is picked up until saltation ceases and a period of rest on the bed, i.e., the rest period, begins. On the basis of experiments [*Einstein*, 1937], *Einstein* [1950] proposes that the average step length is a linear function of the grain diameter:

$$\Lambda = \alpha d, \tag{9}$$

where d denotes the grain size and α denotes the dimensionless step length. For uniform sediment, *Einstein* [1937] and *Fernandez-Luque and Van Beek* [1976] found that α is a constant equal to 100 and 288, respectively. *Yalin* [1977] and others suggest that α slightly increases with increasing shear stress. For nonuniform sediment, *Tsujimoto* [1990] found that the dimensionless step length increases from 10 to 50 with increasing shear stress. For simplicity, we assume the dimensionless step length to be independent of shear stress, whence it is not affected by the variation of shear stress over the stoss face. In addition, we assume the step length small compared to the stoss length so that we may neglect the reduction in step length when a particle falls over the crest of the bed form.

[14] Let us first consider the relation among entrainment, deposition, bed load transport, and step length in more detail. For uniform sediment and after [*Nakagawa and Tsujimoto*, 1980], *Parker et al.* [2000] give the fundamental relations between the deposition rate D and the entrainment rate E and between the bed load transport rate q and the entrainment rate E:

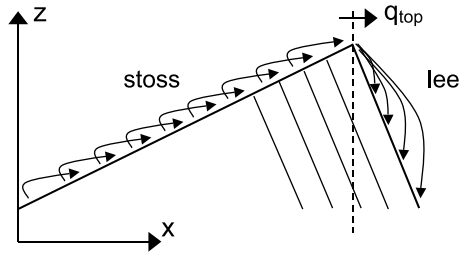

Figure 3. Division of bed form into stoss and lee sides, with accompanying entrainment and deposition fluxes.

$$D(x) = \int_{-\infty}^{x} E(y)\, f_p(x-y)dy \tag{10}$$

$$q(x) = \int_{-\infty}^{x} \left[E(y) \int_{x-y}^{\infty} f_p(y')\, dy' \right] dy, \tag{11}$$

where $f_p(\xi)$ denotes the probability density that a particle, once it is entrained, travels a distance ξ. Equation (10) expresses that a particle is deposited at x when it has been entrained a certain distance upstream from x multiplied by the probability density that its step length is equal to this distance. Equation (11) expresses that a particle passes a cross section at x when it has been entrained a certain distance upstream from x multiplied by the probability density that its step length is equal to or larger than this distance. *Tsujimoto and Motohashi* [1990] propose a relation for the PDF of step lengths, f_p, for plane bed conditions and uniform sediment. For simplicity, we assume the step length to be a deterministic parameter so that f_p reduces to the Dirac delta function and equations (10) and (11) yield

$$D(x) = E(x-\Lambda) \tag{12}$$

$$q(x) = \int_{x-\Lambda}^{x} E(y)\, dy. \tag{13}$$

Equation (12) expresses that the deposition rate at a certain point on the stoss face equals the entrainment rate one step length upstream of this point. Equation (13) expresses that sediment passing the cross section at x has been picked up between x and one step length upstream of x. If the entrainment rate E does not vary significantly within the distance of one step length Λ, equation (13) reduces to

$$q(x) = \Lambda E\left(x - \frac{1}{2}\Lambda\right) \simeq \Lambda E(x). \tag{14}$$

This relation was first used by *Einstein* [1950].

[15] We now return to nonuniform sediment. Let the weighted entrainment rate $E_{si}(x)$ denote the volume of

sediment of grain size d_i locally entrained from the stoss face per unit area and time:

$$E_{si}(x) = E_{siu}(x)\, F_i(x), \tag{15}$$

where x denotes the horizontal coordinate on the scale of a single bed form (Figure 3) and the subscript s indicates the stoss face. The subscript u indicates the case of sediment of only this size fraction. Equation (15) expresses that the entrainment of size fraction i at coordinate x equals the entrainment as if it were uniform sediment of grain size d_i multiplied by its proportion at the bed surface at x. This is comparable to calculating the transport rate of size fraction i in a sediment mixture using $q_i = F_i q_{iu}$, where q_{iu}, like E_{siu}, may include hiding exposure effects. Equation (12) tells us that at the stoss face the weighted deposition rate D_{si} of size fraction i at x equals the weighted entrainment rate of this size fraction one step length upstream of x:

$$D_{si}(x) = E_{siu}(x - \Lambda_i)\, F_i(x - \Lambda_i) \tag{16}$$

where

$$\Lambda_i = \alpha\, d_i \tag{17}$$

$$E_{siu}(x) = 0 \text{ for } x < 0. \tag{18}$$

Similar to equation (13), the local bed load transport rate of size fraction i at the stoss face is given by

$$q_{si}(x) = \int_0^{\Lambda_i} E_{siu}(x - y) F_i(x - y)\, dy \tag{19}$$

$$q_s(x) = \sum_i^N q_{si}(x), \tag{20}$$

where $q_{si}(x)$ denotes the transport rate of size fraction i at coordinate x at the stoss face ($q_{si} = q_s F_{qsi}$), $q_s(x)$ denotes the total transport rate at coordinate x at the stoss face, and $F_{qsi}(x)$ denotes the volume fraction content of size fraction i in the transported mixture at coordinate x at the stoss face.

[16] The present section has shown how the Einstein step length formulation enables us to relate the grain size-specific deposition rate to the grain size-specific entrainment rate at the stoss face of a bed form.

3.2. Deposition Rate at the Lee Face

[17] In the present section a formulation for the average total deposition rate over the bed form lee face will be derived by applying the sediment continuity equation in equation (8) to the local bed form surface:

$$c_b \frac{\partial \eta(x)}{\partial t} = D(x) - E(x) = -\frac{\partial q(x)}{\partial x}, \tag{21}$$

where $\eta(x)$ denotes the local bed surface elevation. Averaging equation (21) over one bed form yields

$$c_b \frac{\partial \eta_a}{\partial t} = -\frac{\lambda_s}{\lambda} E_{s\text{net}} + \frac{\lambda_l}{\lambda} D_l = -\frac{\partial q_a}{\partial x}, \tag{22}$$

wherein entrainment on the lee face is neglected and where λ denotes the bed form length, λ_s denotes the horizontal length of the stoss face, λ_l denotes the horizontal length of the lee face, D_l denotes the average total deposition rate on the lee face, and $E_{s\text{net}}$ denotes the net entrainment rate on the stoss face, which will be discussed in the next paragraph. The bed form-averaged transport rate is given by $q_a = (1/\lambda) \int_0^{\lambda} q(x)\, dx$, and the bed form-averaged bed level is given by $\eta_a = (1/\lambda) \int_0^{\lambda} \eta(x)\, dx$. Note that the average transport rate, q_a, and the mean bed level, η_a, are here defined as averaged over a single bed form. They can still show a spatial variation between bed forms, as suggested by equation (22).

[18] The net entrainment rate on the stoss face, $E_{s\text{net}}$, equals

$$\begin{aligned} E_{s\text{net}} &= \frac{1}{\lambda_s} \sum_i^N \int_0^{\lambda_s} (E_{si}(x) - D_{si}(x))\, dx \\ &= \frac{1}{\lambda_s} \sum_i^N \left[\int_0^{\lambda_s} E_{siu}(x) F_i(x)\, dx - \int_{-\Lambda_i}^{\lambda_s - \Lambda_i} E_{siu}(x) F_i(x)\, dx \right], \end{aligned} \tag{23}$$

which is found by introducing equation (16). Consistent with equation (18), we neglect the contribution from $-\Lambda_i$ to 0 in the second integral so that equation (23) reduces to

$$E_{s\text{net}} = \frac{1}{\lambda_s} \sum_i^N \int_{\lambda_s - \Lambda_i}^{\lambda_s} E_{siu} F_i\, dx. \tag{24}$$

Comparison of equation (24) with equations (19) and (20) shows that the total rate of sediment transport approaching the bed form crest, q_{top}, is related to the net entrainment rate, $E_{s\text{net}}$, in the following way:

$$q_{\text{top}} = \lambda_s E_{s\text{net}}, \tag{25}$$

in which

$$q_{\text{top}i} = \int_0^{\Lambda_i} E_{siu}(\lambda_s - y) F_i(\lambda_s - y) dy, \tag{26}$$

$$q_{\text{top}} = \sum_i^N q_{\text{top}i}, \qquad F_{\text{top}i} = \frac{q_{\text{top}i}}{q_{\text{top}}}, \tag{27}$$

where $q_{\text{top}}(x, t)$ denotes the total bed load transport rate at the bed form crest, $q_{\text{top}i}(x, t)$ denotes the bed load transport rate of size fraction i at the bed form crest, and $F_{\text{top}i}(x, t)$ denotes the volume fraction content of size fraction i in the sediment transported over the bed form crest. Using equation (25), equation (22) can be written as

$$\lambda_l D_l = q_{\text{top}} - \lambda \frac{\partial q_a}{\partial x}, \tag{28}$$

which tells us that the average lee face deposition rate is determined by (1) the net entrainment rate on the stoss face (which equals the amount of sediment transported over the crest divided over the length of the stoss face) and (2) the divergence in the total bed load transport rate.

[19] Thus equation (28) provides another component of the formulations for the vertical sorting fluxes required for the new continuum sorting model: the formulation for the average total deposition rate over the lee face.

3.3. Composition of the Lee Face Deposit

[20] Now, we need to find a formulation for the composition of the lee face deposit. For this purpose, we again apply the sediment continuity equation (8) to the local bed form surface, yet now we consider only a single size fraction:

$$D_i(x) - E_i(x) = -\frac{\partial q_i(x)}{\partial x}, \tag{29}$$

where D_i, E_i, and q_i are related to D, E, and q according to $D = \sum_i^N D_i$, $E = \sum_i^N E_i$ and $q = \sum_i^N q_i$. Averaging equation (29) over one bed form yields

$$\frac{1}{\lambda}\int_0^{\lambda_s} (D_{si}(x) - E_{si}(x))\, dx + \frac{\lambda_l}{\lambda} D_l F_{\mathrm{lee}i} = -\frac{\partial q_{ai}}{\partial x}, \tag{30}$$

which, using equations (23) and (25), can be reformulated to

$$F_{\mathrm{lee}i} = \frac{1}{\lambda_l D_l}\left(q_{\mathrm{top}i} - \lambda \frac{\partial q_{ai}}{\partial x}\right), \tag{31}$$

where $F_{\mathrm{lee}i}$ denotes the volume fraction content of size fraction i in the deposit at the bed form lee face, q_{ai} denotes the bed form-averaged bed load transport rate of size fraction i ($q_{ai} = F_{ai} q_a$), and F_{ai} denotes the bed form-averaged volume fraction content of size fraction i in the bed load transport. Equation (31) tells us that the composition of the lee face deposit, $F_{\mathrm{lee}i}$, is determined by (1) the composition of sediment transported over the bed form crest and by (2) the divergence in the bed load transport of size fractions.

[21] In order to solve for the average total deposition rate over the bed form lee face, D_l, in equation (28) and the composition of the lee face deposit, $F_{\mathrm{lee}i}$, in equation (31), we need a formulation for the average bed load transport rate of size fraction i, q_{ai}. For that purpose, we first consider the transport rate over the lee face and apply equation (21) to the bed form lee face. We assume the lee face of each bed form to have a uniform slope and apply the simple wave theory to bed form migration [*Bagnold*, 1941], which yields that D_l is uniform over the lee face ($D_l(x) = D_l = -\partial q_l/\partial x$). As a boundary condition, we assume that the transport rate is equal to zero at the trough ($q_l = 0$ at $x = \lambda$), which results in

$$q_l(x) = (\lambda - x) D_l \tag{32}$$

$$q_{lai} = \frac{1}{2} D_l \lambda_l F_{\mathrm{lee}i}. \tag{33}$$

In reality, in the average transport rate of size fraction i over the lee face, q_{lai}, there will be a slight bias toward the coarser particles since, on average, they will be transported farther down the lee face than the finer ones. For simplicity, this has been neglected. The bed form-averaged bed load transport rate of size fraction i, q_{ai}, is then obtained by using equation (19) for the stoss face and equation (33) for the lee face:

$$q_{ai} = \frac{1}{\lambda}\int_0^{\lambda_s}\int_0^{\Lambda_i} E_{siu}(x-y) F_i(x-y)\, dy\, dx + \frac{\lambda_l}{2\lambda} D_l \lambda_l F_{\mathrm{lee}i}, \tag{34}$$

$$q_a = \sum_i^N q_{ai}, \qquad F_{ai} = \frac{q_{ai}}{q_a}. \tag{35}$$

Using equations (31), (28), and (35), we are now able to solve for the composition of the total lee face deposit. As a next step, we need to develop a lee sorting function that describes how the size fractions in the lee deposit are distributed over the bed form lee face. First, the present formulations dependent on x will be transformed into formulations dependent on z.

3.4. Elevation-Specific Formulations

[22] Since formulations in the PPL framework are elevation-specific, we need to transform the formulations derived in the previous few sections into formulations dependent on bed elevation z. Appendix B shows in detail how $q_{\mathrm{top}i}$ in equation (26) and q_{ai} in equation (34) can be written as equations (B16) and (B17):

$$q_{\mathrm{top}i} = \lambda_s \int_{\eta_l - \eta_{\mathrm{step}i}}^{\eta_l} E_{siu}(z) F_i(z) p_{se}(z) dz$$

$$q_{ai} = \frac{\lambda_s^2}{\lambda}\int_{\eta_b}^{\eta_l}\int_0^{\eta_{\mathrm{step}i}} E_{siu}(z-z') F_i(z-z') p_{se}(z) p_{se}(z') dz' dz + \frac{\lambda_l}{2\lambda} D_l \lambda_l F_{\mathrm{lee}i}.$$

[23] Thus we have converted the formulations previously written as a function of the coordinate x into formulations dependent on bed elevation z so as to make them suitable for being incorporated into the PPL framework.

3.5. Lee Sorting Function

[24] In the present section we will derive a formulation for the grain size-specific deposition down the bed form lee face. To that end, we introduce the quantity $F_{\mathrm{leeloc}i}(z, t)$, which denotes the volume fraction content of size fraction i in the sediment deposited at elevation z at the bed form lee face. The amount of sediment of size fraction i deposited at elevation z at the lee face then equals $D_l F_{\mathrm{leeloc}i}(z)$. We define $F_{\mathrm{leeloc}i}$ as

$$F_{\mathrm{leeloc}i} = F_{\mathrm{lee}i}\, \omega_i, \tag{36}$$

where $\omega_i(z)$ is the lee sorting function, which determines to what extent a specific size fraction that is transported over the bed form crest is deposited at a certain elevation of the lee face. A first constraint to the lee sorting function is that integration of the composition of the deposited sediment over the lee face, $F_{\mathrm{leeloc}i}$, must result in the composition of the lee face deposit, $F_{\mathrm{lee}i}$:

$$F_{\mathrm{lee}i} = \frac{1}{\lambda_l}\int_{\lambda_s}^{\lambda} F_{\mathrm{leeloc}i}\, dx, \tag{37}$$

where $\sum_i^N F_{\mathrm{leeloc}i} = 1$ and $0 \le F_{\mathrm{leeloc}i} \le 1$.

[25] Generally, the fine size fractions in a sediment mixture prefer to be deposited at the upper parts of the lee face and the coarse size fractions at its lower parts [*Blom et al.*, 2003; *Kleinhans*, 2004]. On the basis of these insights, we now assume that the coarse size fraction is distributed over this uniformly sloped lee face with its volume fraction content decreasing linearly with elevation:

$$\omega_i = J(1 + \delta_i \hat{z}^*), \tag{38}$$

where J (z) is a Heaviside function which equals 1 when considering an elevation covered by the specific bed form (Appendix B). The lee sorting parameter δ_i is a grain size-specific constant, which will be considered in detail in the next few paragraphs, and $\hat{z}^*$ is a dimensionless vertical coordinate relative to the average elevation of the lee face:

$$\hat{z}^* = z^* - \frac{1}{2} - \eta_b^*; \tag{39}$$

by definition, $\hat{z}^* = -(1/2)$ at the lower limit of the lee face (where $z^* = \eta_b^*$) and $\hat{z}^* = (1/2)$ at the upper limit of the lee face (where $z^* = \eta_t^*$). It can be found that equation (38) together with equation (36) indeed meets the constraint in equation (37).

[26] In order to have the δ_i submodel capture the principal effects of lee sorting, the authors believe that the submodel should at least incorporate the effects of (1) the difference in grain size between size fraction i and the geometric mean grain size of the lee deposit, expressed by $\phi_{m\text{lee}} - \phi_i$; (2) the arithmetic standard deviation of the lee deposit, σ_a; and (3) the dimensionless bed shear stress, τ_b^*.

[27] It is likely that the larger the difference in grain size between a specific size fraction i and the geometric mean grain size of the lee deposit ($\phi_{m\text{lee}} - \phi_i$), the larger the effect is of grain sorting at the lee face and thus the larger δ_i should be (see Figure 4).

[28] To understand the effect of the gradation of the mixture, specified by σ_a, we consider one specific grain size ϕ_i in two mixtures: a widely graded mixture and a narrowly graded mixture (Figure 5). The two mixtures are characterized by identical geometric mean grain sizes of the lee deposit, $\phi_{m\text{lee}}$. In this example, size fraction i is finer

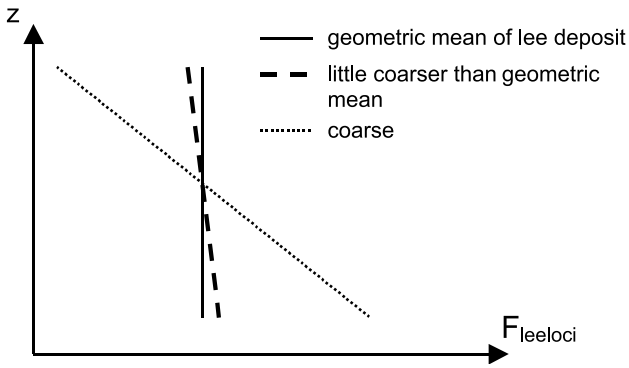

Figure 4. Lee sorting of three size fractions in one sediment mixture.

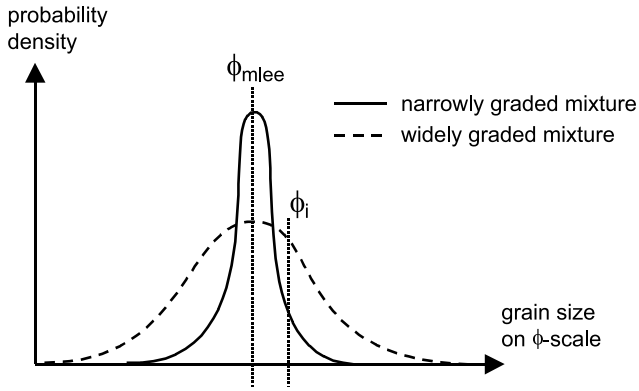

Figure 5. Influence of the gradation of a mixture on sorting at the lee face.

than the geometric mean grain size of the lee deposit. Namely, the larger the grain size on ϕ scale, the smaller is the grain size d_i. Figure 5 illustrates why for the widely graded mixture, the sorting of size fraction i at the lee face will be less than in the narrowly graded mixture, despite the difference between $\phi_{m\text{lee}}$ and ϕ_i for the two mixtures being identical. This is caused by size fraction i being relatively closer to the geometric mean grain size for the widely graded mixture, due to its larger gradation. For the widely graded mixture the amount of size fractions finer than size fraction i is larger and these all need to be deposited in the upper part of the lee face.

[29] *Allen* [1965] and *Kleinhans* [2002] have shown that the lee face sorting trend becomes smaller with increasing shear stress.

[30] On the basis of these considerations and as a first step, the authors propose the following formulation for the lee sorting parameter δ_i:

$$\delta_i = -\gamma \frac{\phi_{m\text{lee}} - \phi_i}{\sigma_a} (\tau_b^*)^{-\kappa}, \tag{40}$$

where

$$\phi_{m\text{lee}} = \sum_i^N \phi_i F_{\text{lee}i}, \tag{41}$$

$$\sigma_a^2 = \sum_i^N (\phi_i - \phi_{m\text{lee}})^2 F_{\text{lee}i}, \tag{42}$$

$$\tau_b^* = \tau_b / [(\rho_s - \rho) g d_{m\text{lee}}], \tag{43}$$

$$d_{m\text{lee}} = \frac{1}{1000}\, 2^{-\phi_{m\text{lee}}}, \tag{44}$$

where $d_{m\text{lee}}$ denotes the geometric mean grain size of the lee deposit in meters, $\phi_{m\text{lee}}$ denotes the geometric mean grain size of the lee deposit on ϕ scale, ϕ_i denotes the grain size of size fraction i on ϕ scale ($\phi_i = -^2\log 1000\ d_i$ with d_i in meters), and τ_b^* denotes the dimensionless bed shear stress averaged over the bed form length. The constant γ weights

the relative importance of the grain size term on the right-hand side of equation (40), while the value of κ sets the relative importance of the dimensionless bed shear stress term. Section 6 will show some general results of the lee sorting function.

[31] Finally, we consider two bed forms having different bed form heights and assume that the sediment transported over their crests is identical in composition. The formulation for $F_{\mathrm{leeloc}i}$ in equations (36) and (38) implies that at the lower (and upper) boundaries of the two bed forms the volume fraction content of each size fraction in the deposit is identical. It implies that the sorting trend becomes stronger with decreasing bed form height. Studying the sorting process of sediment over a delta face (i.e., at a sudden and large transition in water depth), *Kleinhans* [2002] indeed found that the delta height has little influence on the volume fraction content of size fractions deposited at the upper and lower boundaries of the delta front.

[32] In summary, we propose a new simple trend-based lee sorting function meant for deriving a formulation for the grain size-specific deposition over the bed form lee face. It seems to be the simplest form of a lee face sorting model that has any hope of capturing the effects in question.

4. PPL Framework and Bed Form Migration Approach

4.1. Regular Bed Form Size

[33] In the present section the bed form migration approach will be coupled to the Parker-Paola-Leclair framework for sediment continuity. We first convert the entrainment and deposition rates as used in the bed form migration approach into entrainment and deposition densities as used in this framework. Subsequently, in section 4.2 we incorporate the irregularities of bed forms by taking into account the stochastic nature of the trough elevations.

[34] In section 3 we distinguished an entrainment flux at the stoss face, a deposition flux at the stoss face, and a deposition flux at the lee face so that we rewrite the right-hand terms in the fundamental equation of the PPL framework, equation (5):

$$c_b\bar{P}_s(z)\frac{\partial\bar{F}_i(z)}{\partial t}+c_b\bar{F}_i(z)\frac{\partial\tilde{P}_s(z)}{\partial t}+c_b\bar{F}_i(z)\bar{p}_e(z)\frac{\partial\bar{\eta}_a}{\partial t}=\bar{D}_{eis}(z)-\bar{E}_{eis}(z)+\bar{D}_{eil}(z), \tag{45}$$

where $\bar{E}_{eis}$, $\bar{D}_{eis}$, and $\bar{D}_{eil}$ denote the entrainment density of size fraction i on the stoss face, the deposition density on the stoss face, and the deposition density on the lee face, respectively. For clarity, equation (45) only shows the argument in the z direction and leaves out the arguments x and t.

[35] Note that in the present section we deal with series of regular bed forms so that the parameters averaged over a series of bed forms are simply identical to the corresponding parameters for a single bed form, e.g.,

$$\bar{F}_i(z)=F_i(z),\qquad \bar{E}_{siu}(z)=E_{siu}(z),$$

$$\bar{F}_{\mathrm{leeloc}i}(z)=F_{\mathrm{leeloc}i}(z),\qquad \bar{\lambda}_s=\lambda_s,$$

$$\bar{p}_{se}(z)=p_{se}(z).$$

Now, let us consider the relation between the entrainment density $\bar{E}_{eis}$ in equation (45) and the entrainment rate $\bar{E}_{siu}$. The entrainment rate $\bar{E}_{siu}$ is defined as the volume of sediment of size fraction i picked up from the bed per unit length, width, and time, in case only size fraction i is present. As explained near equation (15), $\bar{E}_{siu}$ may include hiding exposure effects. Thus the volume of sediment of size fraction i picked up from the stoss face from a bed layer with a thickness dz_s per unit width and time equals

$$\bar{E}_{siu}(z)\bar{F}_i(z)dx_s, \tag{46}$$

where dx_s is the horizontal extent over which the bed layer with thickness dz_s is exposed to the flow at the stoss face. According to equation (B13), dx_s can be written as

$$dx_s=\bar{\lambda}_s\bar{p}_{se}(z)\,dz.$$

The entrainment density $\bar{E}_{eis}$ of size fraction i is defined such that $\bar{E}_{eis}\,dxdz$ is the volume of size fraction i entrained from a bed element with sides dx and dz at elevation z at the stoss face, per unit width and time. Thus the entrainment density at the stoss face equals

$$\begin{aligned}\bar{E}_{eis}(z)&=\frac{\bar{E}_{siu}(z)\bar{F}_i(z)\bar{\lambda}_s\bar{p}_{se}(z)\,dz}{\bar{\lambda}\,dz}\\&=\frac{\bar{\lambda}_s}{\bar{\lambda}}\bar{p}_{se}(z)\bar{E}_{siu}(z)\bar{F}_i(z).\end{aligned} \tag{47}$$

Then, in accordance with the Einstein step length formulation, the deposition density at the stoss face

$$\bar{D}_{eis}(z)=\frac{\bar{\lambda}_s}{\bar{\lambda}}\bar{p}_{se}(z)\bar{E}_{siu}\Big(z-\eta_{\mathrm{step}i}(z)\Big)\,\bar{F}_i\Big(z-\eta_{\mathrm{step}i}(z)\Big), \tag{48}$$

and the deposition density at the lee face

$$\bar{D}_{eil}(z)=\frac{\bar{\lambda}_l}{\bar{\lambda}}\bar{p}_{le}(z)\bar{D}_l\bar{F}_{\mathrm{leeloc}i}(z), \tag{49}$$

where $\bar{F}_{\mathrm{leeloc}i}$ allows for grain size sorting down the avalanche lee face (section 3.5). The bed load transport rate of size fraction i averaged over the series of bed forms, $\bar{q}_{ai}$, equals q_{ai} in equation (B17). Likewise, the bed load transport rate of size fraction i over the bed form crest and averaged over the series of bed forms, $\bar{q}_{\mathrm{top}i}$, equals $q_{\mathrm{top}i}$ in equation (B16).

[36] Thus we have coupled the single bed form migration approach to the PPL framework for sediment continuity, but the resulting set of equations is still only valid for a series of regular dunes. In reality, the variation of bed form geometry can be large, which gives rise to vertical sorting fluxes at bed elevations that are only reached by bed forms with very deep troughs.

4.2. Irregular Bed Form Size

[37] In this section the irregularities in bed form size are taken into account by incorporating the statistics of the trough elevations. We suppose that each individual bed form in a series of irregular bed forms is characterized by the vertical distance from its trough to the mean bed level.

The latter is also indicated in terms of the relative trough elevation Δ_b ($\Delta_b = \bar{\eta}_a - \eta_b$). The PDF of relative trough elevations is given by $\tilde{p}_{\eta_b}$. Note that all bed forms in the series are assumed to have the same characteristic shape, expressed by the dimensionless PDFs of bed surface elevations for the stoss and the lee face, $\bar{p}^*_{se}$ and $\bar{p}^*_{le}$, respectively. As mentioned in section 3.3, each lee face is assumed to have a uniform slope so that $\bar{p}^*_{le} = J$. Note that the term irregular bed forms refers to irregularity in bed form dimensions but not in shape. All bed form-specific features, e.g., bed form height and bed form length, are assumed to be simply related to the relative trough elevation by

$$\Delta = 2\Delta_b, \tag{50}$$

$$\lambda = (\lambda_a/\Delta_a)\Delta, \tag{51}$$

$$\lambda_l = \Delta/\tan(\nu), \tag{52}$$

$$\lambda_s = \lambda - \lambda_l, \tag{53}$$

where Δ_a denotes the average bed form height and λ_a denotes the average bed form length. (Also see Figure 6 for the definition of these parameters.) The crests of the bed forms are assumed to have the same absolute distance to the mean bed level as the troughs, and the steepness of the lee faces is assumed to be equal to the angle of repose (ν). The bed form length is assumed to be proportional to the bed form height, and the ratio of the average bed form length is assumed to be equal to the average bed form height.

[38] One may rightfully claim that the parameters Δ, λ, and λ_l may be related to the relative trough elevation in a way different from equations (50)–(52). The purpose of these formulations is to account for the irregularity of bed forms in a relatively simple way so that the method can be incorporated in the new continuum sorting model. Equations (50)–(52) are not supposed to be generally valid, and when applying these formulations, their applicability should be checked against data. Note that the following part of the paper is also valid if equations (50)–(52) were not applicable.

[39] Let us now address the procedure of averaging some general bed form-specific parameter, μ, over a series of irregular bed forms. This requires the parameter to be weighted by the proportion of the total length of the series of bed forms that is related to a specific relative trough elevation. Yet the PDF of relative trough elevations, $\tilde{p}_{\eta_b}$, only expresses the likelihood that a certain trough elevation occurs and not what proportion of the total length of the series of bed forms is involved. Therefore, in averaging some general bed form-specific parameter, μ, over various bed forms, it should not only be weighted by the probability density that a specific relative trough elevation occurs but also by the bed form length:

$$\bar{\mu} = \frac{1}{\hat{\lambda}} \int_{\eta_{b\min}}^{\eta_{b\max}} \lambda\, \mu\, \tilde{p}_{\eta_b}\, d\eta_b, \tag{54}$$

where $\bar{\mu}$ is called the overall parameter μ. The weighted bed form length, $\hat{\lambda}$, normalizes equation (54), and

$$\hat{\lambda} = \int_{\eta_{b\min}}^{\eta_{b\max}} \lambda\, \tilde{p}_{\eta_b}\, d\eta_b. \tag{55}$$

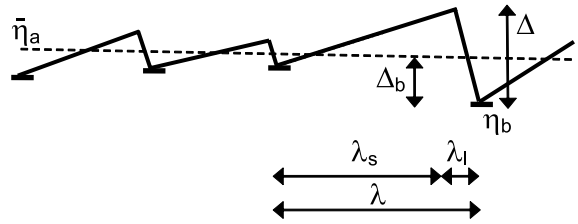

Figure 6. Bed form parameters. For clarity, the bed forms are here assumed to have a triangular shape.

For clarity, we now define an adapted PDF of relative trough elevations, $\tilde{p}_b$, which equals the PDF of relative trough elevations, $\tilde{p}_{\eta_b}$, weighted by the proportion of the total length of the series of bed forms that is related to a specific relative trough elevation:

$$\tilde{p}_b = \frac{\lambda}{\hat{\lambda}} \tilde{p}_{\eta_b} \tag{56}$$

so that the overall parameter μ in equation (54) can be rephrased to

$$\bar{\mu} = \int_{\eta_{b\min}}^{\eta_{b\max}} \mu\, \tilde{p}_b\, d\eta_b. \tag{57}$$

[40] Likewise, using equations (B6) and (B4), we find that the overall PDF of bed surface elevations, $\bar{p}_e$, is now determined by the characteristic bed form shape, $\bar{p}^*_{se}$, and by the PDF of relative trough elevations, $\tilde{p}_b$, according to

$$\begin{aligned} \bar{p}_e(z) &= \int_{\eta_{b\min}}^{\eta_{b\max}} p_e(z)\tilde{p}_b\, d\eta_b \\ &= \int_{\eta_{b\min}}^{\eta_{b\max}} \frac{J(z)}{\lambda\Delta} (\lambda_s \bar{p}^*_{se}(z) + \lambda_l)\, \tilde{p}_b\, d\eta_b, \end{aligned} \tag{58}$$

where J, Δ, λ, λ_s, and λ_l are all related to the specific relative trough elevation, Δ_b. The overall probability distribution of bed surface elevations, $\bar{P}_s$, is given by equation (2).

[41] The derivation of the entrainment and deposition densities averaged over a series of irregular bed forms ($\bar{E}_{eis}$, $\bar{D}_{eis}$, and $\bar{D}_{eil}$) is similar to those for regular bed forms, given by equations (47), (48), and (49). Yet we now average the right-hand terms over all trough elevations:

$$\bar{E}_{eis}(z) = \int_{\eta_{b\min}}^{\eta_{b\max}} \frac{\lambda_s}{\lambda} p_{se}(z) E_{siu}(z)\, \bar{F}_i(z)\, \tilde{p}_b d\eta_b, \tag{59}$$

$$\begin{aligned} \bar{D}_{eis}(z) = \int_{\eta_{b\min}}^{\eta_{b\max}} & \frac{\lambda_s}{\lambda} p_{se}(z) E_{siu}\Big(z - \eta_{\text{step}i}(z)\Big) \\ & \cdot \bar{F}_i\Big(z - \eta_{\text{step}i}(z)\Big) \tilde{p}_b\, d\eta_b, \end{aligned} \tag{60}$$

$$\bar{D}_{eil}(z) = \int_{\eta_{b\min}}^{\eta_{b\max}} \frac{\lambda_l}{\lambda} p_{le}(z) D_l\, F_{\text{leeloc}i}(z) \tilde{p}_b\, d\eta_b. \tag{61}$$

Herein we assume that the vertical sorting profile within an individual bed form, F_i, is identical to the sorting profile averaged over the series of bed forms, $\bar{F}_i$. We now find the average bed load transport rate of size fraction i, $\bar{q}_{ai}$, and the average sediment transport over the bed form crest, $\bar{q}_{\text{top}i}$, by

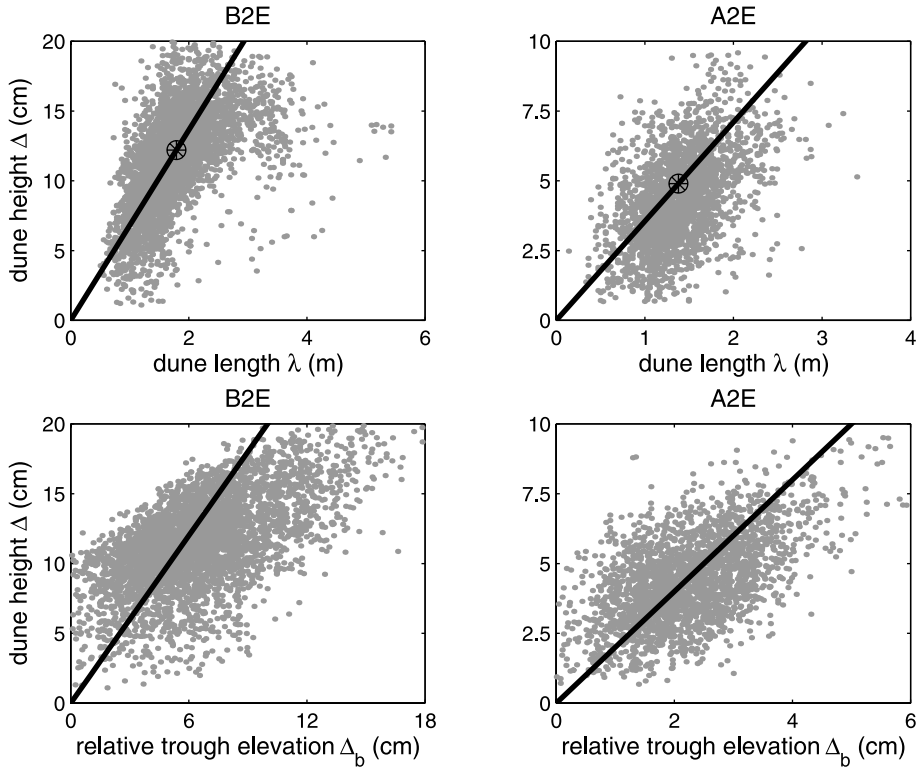

Figure 7. (top) Relation between (1) measured bed form lengths and bed form heights for individual bed forms (small dots), (2) the average the bed form length, λ_a, and the average bed form height, Δ_a (large dot), and (3) the bed form length and bed form height according to equation (51) (line). (bottom) Relation between (1) measured relative trough elevations and bed form heights for individual bed forms (small dots) and (2) the relative trough elevation and bed form height according to equation (50) (line).

averaging q_{ai} in equation (B17) and $q_{\mathrm{top}i}$ in equation (B16) over all trough elevations:

$$\bar{q}_{ai} = \int_{\eta_{b\min}}^{\eta_{b\max}} q_{ai}\, \tilde{p}_b\, d\eta_b \tag{62}$$

$$\bar{q}_{\mathrm{top}i} = \int_{\eta_{b\min}}^{\eta_{b\max}} q_{\mathrm{top}i}\, \tilde{p}_b\, d\eta_b. \tag{63}$$

[42] Thus we have coupled the single bed form migration approach to the PPL framework for sediment continuity for a series of irregularly sized bed forms. The result of section 4 is a new continuum sorting model for bed form-dominated conditions, although the model still lacks a submodel for the grain size-specific entrainment over the stoss face of a bed form.

5. Simplified Continuum Sorting Models

[43] In order to be able to compute the time evolution of the sorting profile, $\bar{F}_i$, and the mean bed level, $\bar{\eta}_a$, we need to make the set of equations complete. A straightforward way to do so would be to acquire a submodel for the grain size-selective entrainment rate over bed forms. As far as is known to the authors, *Tsujimoto* [1990] was the only one who developed an entrainment model especially for nonuniform sediment. Unfortunately, this entrainment model has never been verified for a wide range of conditions, and it is not known whether it gives a good description of entrainment along bed forms as flow patterns over bed forms are strongly nonuniform and very complex. Another source of uncertainty is the variation of a representative measure for the skin friction over the stoss face, which is not easily determined. Moreover, *McLean et al.* [1994] experimentally found that the sediment transport rate over a bed form does not directly depend on the variation of the mean bed shear stress over it. They argue that the sediment transport rate should be related to the statistics of the near-bed turbulence as lift and drag forces on grains are directly related to instantaneously fluctuating velocities.

[44] As it is questionable whether an entrainment model based on mean skin friction would give satisfactory results in predicting the size-selective entrainment rate over the stoss face, it was decided to take on another approach, which is explained in detail by *Blom* [2003] as well as in two follow-up papers (A. Blom et al., manuscripts in preparation, 2004). For equilibrium conditions ($\partial/\partial t = 0$) the continuum sorting model is reduced to an equilibrium sorting model. For nonequilibrium conditions the continuum sorting model is reduced to a relaxation-type sorting evolution model. It solves for the time evolution of both the vertical sorting profile and the composition of the bed load transport from the initial sorting profile, the total bed load transport rate, and the

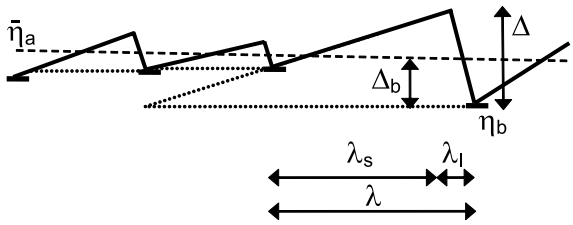

Figure 8. Influence of adjacent bed forms upon the bed form length.

PDF of relative trough elevations. In addition, methods are proposed to account for vertical sediment fluxes through both a change in time of the PDF of relative trough elevations and net aggradation or degradation.

6. Results of Submodels

[45] As the continuum sorting model needs to be reduced to either the equilibrium sorting model or the sorting evolution model first, we can not yet show results of the full continuum sorting model. We do show some results of the submodels of bed form size as well as some general results of the submodel for lee-side sorting. In this section we consider the equilibrium phases of experiments B2 and A2 described by *Blom et al.* [2003]. During these experiments, uniform conditions were maintained ($\partial/\partial x = 0$), and the transported sediment was recirculated in order to avoid net aggradation or degradation over the length of the flume ($\partial\bar{\eta}_a/\partial t = 0$). The sediment mixture consisted of three well-sorted size fractions: $d_{\text{fine}} = 0.68$ mm, $d_{\text{medium}} = 2.1$ mm, and $d_{\text{coarse}} = 5.7$ mm. The sediment transport consisted solely of bed load transport, and the bed was covered by dunes.

[46] First, we study the validity of equations (51) and (50). Figure 7 (top) shows the relation between measured bed form lengths and bed form heights for individual bed forms, together with equation (51). The relation between the measured bed form lengths and bed form heights shows large scatter, but equation (51) covers the possible trend reasonably well. The large scatter seems partly due to the bed form length (i.e., the distance between two consecutive troughs) also being determined by the adjacent bed forms (see Figure 8). Figure 7 (bottom) shows the relation between measured relative trough elevations, Δ_b, and bed form heights, Δ, for individual bed forms. In spite of the large scatter, and although equation (50) deviates from the measured trend for the higher dunes in experiment B2E, equation (50) represents the trend reasonably well.

[47] Secondly, we analyze the sensitivity of the lee-side sorting profile, $F_{\text{leeloc}i}$, to the constants γ and κ in the lee sorting function for experiment A2. It is simply assumed that the composition of the lee face deposit, $F_{\text{lee}i}$, equals the measured average volume fraction contents of the three size fractions in the bed load transport, $\bar{F}_{ai}$, namely 0.38, 0.38, and 0.24. The average bed shear stress was $\bar{\tau}_b = 4.6\ \text{Nm}^{-2}$. First we vary γ over the values $[-1, -0.5, 0.5, 1]$, while κ is set such that the bed shear stress has no effect on the avalanche mechanism at the lee face at all ($\kappa = 0$). Figure 9 (left) shows the resulting computed lee-side sorting profiles for an individual bed form. For

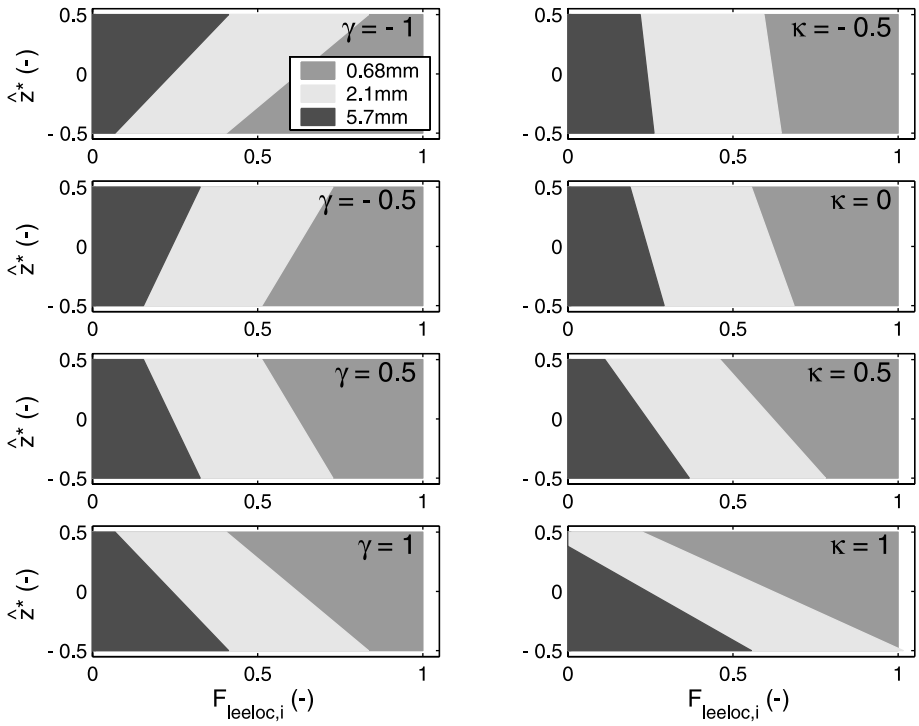

Figure 9. (left) Influence of the constant γ in the lee sorting function on the computed lee-side sorting profile of a single bed form, $F_{\text{leeloc}i}$, while $\kappa = 0$. (right) Influence of the constant κ in the lee sorting function on the computed lee-side sorting profile of a single bed form, $F_{\text{leeloc}i}$, while $\gamma = 0.3$.

negative values of γ the coarse material prefers being deposited at the higher elevations of the active bed. This is contradictory to experimental studies on the avalanche mechanism at the lee face, so we may conclude that γ must have a positive value. Furthermore, it shows that the larger γ, the stronger is the sorting trend in the active bed. To study the effect of κ, we vary κ over the values [−0.5, 0, 0.5, 1], while $\gamma = 0.3$ (see Figure 9 (right)). It clearly shows that the smaller the value for κ, the smaller is the sorting in the active bed. Also, kappa should be positive as the lee face sorting trend is expected to become smaller with increasing shear stress. In the work of *Blom* [2003] and in the first follow-up paper (A. Blom et al., manuscript in preparation, 2004), the constants γ and κ are used as calibration coefficients.

7. Discussion and Conclusions

[48] The authors have developed a new depth-continuous sediment continuity model, which is based on (1) the Parker-Paola-Leclair (PPL) framework; (2) the Einstein step length formulation; (3) a newly developed lee sorting function; and (4) a newly developed method to account for the variability in bed form trough elevations. The present paper presents the derivation of formulations for the grain size-specific and bed elevation-specific entrainment and deposition fluxes as required for the PPL framework. The resulting continuum sorting model incorporates sorting fluxes through (1) the grain size-selective deposition down the avalanche lee face, (2) the variability in bed form trough elevations, and (3) net aggradation or degradation of the river bed.

[49] The present research has focused on the development of a framework for taking into account the effects of vertical sorting in modeling river morphodynamics. The framework contains various submodels (e.g., lee-side sorting; the step length; bed form dimensions; the time evolution of the PDF of trough elevations), which strongly need further development. For instance, the presently proposed lee sorting function still has a very simple form. Also, it would be worthwhile to compare the choice for a deterministic step length to a stochastic one.

[50] In its present form the new continuum sorting model incorporates only bed load transport. Further research is required to also include suspended load transport. Yet a simple way of incorporating suspended load transport is proposed by *Blom* [2003]. Application of the present model should be limited to bed form-dominated conditions. Further study is required to derive formulations for the grain size-specific and elevation-specific entrainment and deposition fluxes under plane bed conditions.

[51] The present paper has explained the derivation of a fundamental mathematical framework for taking into account the impact of vertical sorting upon the large-scale morphodynamics of bed form-dominated rivers. Two follow-up papers (A. Blom et al., manuscripts in preparation, 2004) will consider the simplification of this modeling framework to an equilibrium sorting model and a sorting evolution model, respectively. These follow-up papers will also discuss the application of the reduced models, wherein computed vertical sorting profiles are compared to the vertical sorting, as measured in the experiments by *Blom et al.* [2003], *Ribberink* [1987], and *Kleinhans* [2002]. The performance of the sorting evolution model and the commonly used Hirano active layer model will be compared.

Appendix A: Integral of Time Derivative $\tilde{P}_s$

[52] Near equations (28a) and (28b) in the work of *Parker et al.* [2000], it is argued that the integral $\partial\tilde{P}_s/\partial t$ over z in equation (7) should vanish if $\bar{p}_e$ is symmetric in $\tilde{z}$, i.e., around the mean bed level, $\bar{\eta}_a$. However, the authors found that the integral term in equation (7) should vanish regardless of whether or not $\bar{p}_e$ is symmetric in $\tilde{z}$. Let us consider the integral

$$I = \int_{-r}^{r} \frac{\partial \tilde{P}_s}{\partial t}\, d\tilde{z}, \tag{A1}$$

where $r = \infty$ and where $\tilde{z}$ denotes the bed elevation relative to the mean bed level ($\tilde{z} = z - \bar{\eta}_a\,(x, t)$). We now substitute

$$\bar{P}_s = 1 - \int_{-\infty}^{\tilde{z}} \bar{p}_e\, d\tilde{z}' \tag{A2}$$

into equation (A1),

$$I = -\int_{-r}^{r} \frac{\partial}{\partial t}\left(\int_{-\infty}^{\tilde{z}} \bar{p}_e\, d\tilde{z}'\right) d\tilde{z}, \tag{A3}$$

and rephrase equation (A3) by integrating in parts according to

$$\int g'h = gh\Big| - \int gh', \tag{A4}$$

where

$$g' = 1 \qquad h = -\frac{\partial}{\partial t}\left(\int_{-\infty}^{\tilde{z}} \bar{p}_e\, d\tilde{z}'\right). \tag{A5}$$

This yields

$$I = r\left(\frac{\partial \bar{P}_s}{\partial t}\Big|_r + \frac{\partial \bar{P}_s}{\partial t}\Big|_{-r}\right) + \frac{\partial}{\partial t}\int_{-r}^{r} \tilde{z}\bar{p}_e d\tilde{z}, \tag{A6}$$

wherein the integral term vanishes, as by definition:

$$\int_{-r}^{r} \tilde{z}\, \bar{p}_e\, d\tilde{z} = 0. \tag{A7}$$

In addition, by definition, $\bar{P}_s \to 1$ as $r \to -\infty$ and $\bar{P}_s \to 0$ as $r \to \infty$ so that $\partial\bar{P}_s/\partial t \to 0$ as $r \to \pm\infty$. Under the condition that $\partial\bar{P}_s/\partial t$ converges to 0 faster than r converges to $\pm\infty$ (a condition that holds for, e.g., a Gaussian distribution, in which the standard variation is allowed to vary in time), it is seen that the integral $I \to 0$ as $r \to \infty$, thus demonstrating that the integral term in equation (7) should vanish, regardless of whether or not $\bar{p}_e$ is symmetric in $\tilde{z}$.

Appendix B: Elevation-Specific Formulations

[53] Since formulations in the PPL framework are elevation-specific, we need to transform the formulations depen-

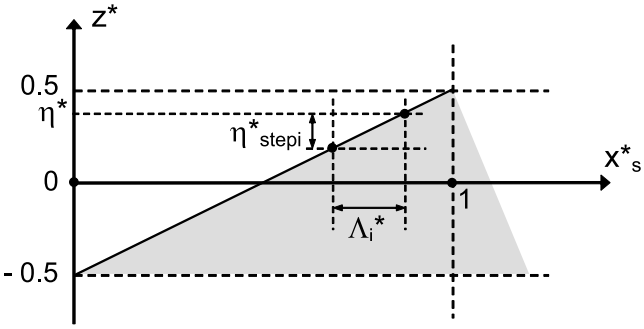

Figure B1. Dimensionless distance of one step length in horizontal and vertical directions for a triangular bed form.

dent on x on bed form scale into formulations dependent on bed elevation z. To that end, we introduce the dimensionless coordinates x_s^*, x_l^*, and z^*:

$$x_s^* = \frac{x}{\lambda_s}, \qquad x_l^* = \frac{x - \lambda_s}{\lambda_l}, \qquad z^* = \frac{z - \eta_a}{\Delta}, \tag{B1}$$

where x_s^* and x_l^* denote the dimensionless horizontal coordinates for the stoss face and lee face, respectively, and z_s^* denotes the dimensionless vertical coordinate. Δ denotes the bed form height, which is given by $\Delta = \eta_t - \eta_b$, where η_b and η_t denote the lower and upper limits of the bed form, respectively. The dimensionless local elevation of the bed surface η is now expressed by

$$\eta^*(x) = \frac{\eta(x) - \eta_a}{\Delta}. \tag{B2}$$

By definition, the dimensionless mean bed level, η_a^*, equals 0. In case the bed form has a triangular shape, the dimensionless lower limit, η_b^*, equals $-(1/2)$, and the upper limit, η_t^*, equals (1/2) (see Figure B1). As we assume each lee face to have a uniform slope, the PDF of active bed elevations at the lee face yields

$$p_{le} = \frac{J}{\Delta}, \qquad J = \begin{cases} 1 & \text{if } \eta_b \le z \le \eta_t, \\ 0 & \text{else,} \end{cases} \tag{B3}$$

where $J(z)$ is a Heaviside function that equals 1 when considering an elevation covered by the specific bed form.

[54] We now define dimensionless PDFs of the bed surface elevations for the stoss side, p_{se}^*, and for the lee side, p_{le}^*:

$$p_{se}^* = \frac{dx_s^*}{d\eta^*} = \Delta p_{se} \tag{B4}$$

$$p_{le}^* = -\frac{dx_l^*}{d\eta^*} = \Delta p_{le}, \tag{B5}$$

where $d\eta^* = d\eta/\Delta$. The bed form-averaged probability density of bed surface elevations is given by

$$p_e = \frac{\lambda_s}{\lambda} p_{se} + \frac{\lambda_l}{\lambda} p_{le} = \frac{J}{\Delta\lambda}(\lambda_s p_{se}^* + \lambda_l). \tag{B6}$$

Like $p_e = -\partial P_s/\partial\eta$ in equation (4), the probability density of bed surface elevations for the stoss face equals

$$p_{se} = -\frac{\partial P_{ss}}{\partial \eta} \tag{B7}$$

$$p_{se}^* = -\frac{\partial P_{ss}}{\partial \eta^*}, \tag{B8}$$

where $P_{ss}(z)$ denotes the probability that the stoss face elevation is higher than z. Now, comparing equation (B8) with equation (B4) and studying the example of a triangular bed form in Figure B2 yields

$$x_s^* = 1 - P_{ss}. \tag{B9}$$

For the stoss face we now introduce the function f_{ds}, which expresses the dimensionless elevation of the stoss face as a function of the dimensionless horizontal coordinate and its inverse, the function g_{ds}:

$$\eta^* = f_{ds}(x_s^*) \tag{B10}$$

$$x_s^* = g_{ds}(\eta^*). \tag{B11}$$

Comparison of equations (B9) and (B11) yields

$$g_{ds} = 1 - P_{ss}. \tag{B12}$$

[55] In order to transform the equations listed in the previous few sections into equations dependent on bed elevation z, we rewrite the integrals over dx, e.g., in equation (26), into integrals over dz. When considering the stoss face, we replace dx by

$$dx = \lambda_s\, dx_s^* = \lambda_s p_{se}^*\, dz^* = \lambda_s p_{se}\, dz. \tag{B13}$$

In addition, we translate the step length Λ_i into a dimensionless vertical step length, $\eta_{\text{step}i}^*$:

$$\eta_{\text{step}i}^* = \eta^* - f_{ds}[g_{ds}(\eta^*) - \Lambda_l^*], \tag{B14}$$

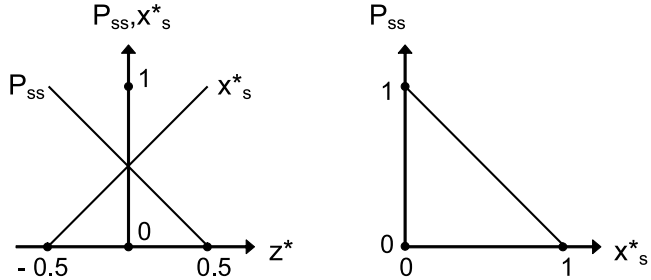

Figure B2. Relation between x_s^* and the probability distribution of bed surface elevations P_{ss} for a triangular bed form.

where $\eta^*_{\text{step}i} = \eta_{\text{step}i}/\Delta$ and $\Lambda^*_i = \Lambda_i/\lambda_s$. This is illustrated in Figure B1. Using equation (B13) to manipulate $q_{\text{top}i}$ in equation (26), we find that

$$q_{\text{top}i} = \lambda_s \int_{\eta_l - \eta_{\text{step}i}}^{\eta_l} E_{siu}\left(\lambda_s g_{ds}\left(\frac{z-\eta_a}{\Delta}\right)\right) F_i\left(\lambda_s g_{ds}\left(\frac{z-\eta_a}{\Delta}\right)\right) \cdot p_{se}\left(\lambda_s g_{ds}\left(\frac{z-\eta_a}{\Delta}\right)\right) dz. \quad \text{(B15)}$$

For clarity, we no longer present the arguments in the parameters E_{siu}, F_i, and p_{se} as x coordinates ($x = \lambda_s g_{ds}((z - \eta_a/\Delta))$), but we abbreviate these functional relations such that $E_{siu}(z)$, $F_i(z)$, and $p_{se}(z)$ are their equivalents, respectively. Then, $q_{\text{top}i}$ in equation (B15) and q_{ai} in equation (34) are written as

$$q_{\text{top}i} = \lambda_s \int_{\eta_l - \eta_{\text{step}i}}^{\eta_l} E_{siu}(z) F_i(z) p_{se}(z)\, dz \quad \text{(B16)}$$

$$q_{ai} = \frac{\lambda_s^2}{\lambda} \int_{\eta_b}^{\eta_l} \int_0^{\eta_{\text{step}i}} E_{siu}(z - z') F_i(z - z') p_{se}(z)\, p_{se}(z') dz'\, dz + \frac{\lambda_l}{2\lambda} D_l \lambda_l F_{\text{lee}i}. \quad \text{(B17)}$$

Notation

$( )^*$ superscript denoting a dimensionless parameter.
$\bar{( )}$ parameter is horizontally averaged over a series of bed forms.
$\tilde{( )}$ parameter is relative to the mean bed level.
c_b sediment concentration within the bed ($c_b = 1 - \lambda_b$).
$\bar{C}_i$ concentration of size fraction i at elevation z, averaged over a series of bed forms.
d_i grain size of size fraction i, m.
$d_{m\text{lee}}$ geometric mean grain size of the lee deposit, m.
$\bar{D}$ volume of deposited sediment per unit area and time, summed over all size fractions and averaged over a series of bed forms, m s^{-1}.
$\bar{D}_e$ deposition density defined like $\bar{D}_{ei}$ but summed over all size fractions, s^{-1}.
$\bar{D}_{ei}$ deposition density of size fraction i defined such that $\bar{D}_{ei}dxdz$ is the volume of size fraction i deposited in a bed element with sides dx and dz at elevation z, per unit width and time, averaged over a series of bed forms, s^{-1}.
D_l deposition rate at the lee face, m s^{-1}.
D_{si} volume of size fraction i locally deposited onto the stoss face, per unit area and time, m s^{-1}.
$\bar{E}$ volume of entrained sediment per unit area and time, summed over all size fractions and averaged over a series of bed forms, m s^{-1}.
$\bar{E}_e$ entrainment density defined like $\bar{E}_{ei}$ but summed over all size fractions, s^{-1}.
$\bar{E}_{ei}$ entrainment density of size fraction i, defined such that $\bar{E}_{ei}dxdz$ is the volume of size fraction i entrained from a bed element with sides dx and dz at elevation z, per unit width and time, averaged over a series of bed forms, s^{-1}.
$E_{s\text{net}}$ net entrained volume of all size fractions on the stoss face, per unit area and time, m s^{-1}.
E_{si} volume of size fraction i locally entrained from the stoss face, per unit area and time, m s^{-1}.
E_{siu} volume of size fraction i locally entrained from the stoss face, per unit area and time, if only sediment of size fraction i would be present, m s^{-1}.
f_{ds} elevation of the stoss face as a function of its horizontal coordinate, dimensionless.
$f_p(\xi)$ probability density that step length equals ξ.
$\bar{F}_{ai}$ volume fraction content of size fraction i in the bed load transport, averaged over a series of bed forms.
$\bar{F}_i$ volume fraction content of size fraction i in the bed at elevation z, averaged over a series of bed forms.
$\bar{F}_{\text{lee}i}$ volume fraction content of size fraction i in the lee deposit, averaged over a series of bed forms.
$F_{\text{leeloc}i}$ volume fraction content of size fraction i in the sediment deposited at elevation z at the lee face.
$\bar{F}_{\text{top}i}$ volume fraction content of size fraction i in the bed load transport over the bed form crest, averaged over a series of bed forms.
g_{ds} horizontal coordinate of the stoss face as a function of its elevation, dimensionless.
$( )_i$ subscript indicating the number of the size fraction.
$J(z)$ Heaviside function, which equals 1 when considering an elevation covered by the bed form.
$( )_l$ subscript indicating the lee face.
N total number of size fractions.
$\tilde{p}_{\eta_b}$ probability density function of trough elevations relative to the mean bed level for a series of bed forms, indicating the probability density that the trough elevation equals z, m^{-1}.
$\tilde{p}_b$ adapted probability density function of trough elevations relative to the mean bed level for a series of bed forms, indicating the probability density that the trough elevation equals z, weighted by the horizontal distance involved, m^{-1}.
$\bar{p}_e$ probability density function of bed surface elevations for a series of bed forms, indicating the probability density that the bed surface elevation equals z, m^{-1}.
$\bar{p}^*_e$ probability density function of bed surface elevations for a series of bed forms, dimensionless.
p_e probability density function of bed surface elevations for an individual bed form, m^{-1}.
$\bar{P}_s$ probability distribution of bed surface elevations for a series of bed forms, indicating the probability that the bed surface elevation is higher than z.
q volume of bed load transport per unit width and time (excluding pores), m^2 s^{-1}.
$\bar{q}_a$ volume of bed load transport per unit width and time (excluding pores), averaged over a series of bed forms, m^2 s^{-1}.
$\bar{q}_{\text{top}}$ volume of bed load transport at the bed form crest per unit width and time (excluding pores), averaged over a series of bed forms, m^2 s^{-1}.
$( )_s$ subscript indicating the stoss face.
t time coordinate, s.
x horizontal coordinate, m.

x^* horizontal coordinate on the scale of an individual bed form, dimensionless.
z vertical coordinate, m.
$\tilde{z}$ vertical coordinate relative to the mean bed level $\bar{\eta}_a$, m.
z^* vertical coordinate relative to the mean bed level $\bar{\eta}_a$, dimensionless.
$\hat{z}^*$ vertical coordinate relative to the mean bed level $\bar{\eta}_a$, dimensionless.
α step length, dimensionless.
γ constant in lee sorting function.
δ_i lee sorting parameter.
Δ bed form height, m.
Δ_a bed form height averaged over a series of bed forms, m.
Δ_b trough elevation relative to the mean bed level, i.e., the relative trough elevation, m.
η local bed surface elevation, m.
η_a bed surface elevation averaged over a single bed form, m.
$\bar{\eta}_a$ bed surface elevation averaged over a series of bed forms (mean bed level), m.
η_b bed form trough elevation, m.
$\eta_{b\max}$ highest bed form trough elevation, m.
$\eta_{b\min}$ lowest bed form trough elevation, m.
η_t bed form crest elevation, m.
$\eta_{\text{step}i}$ step length in z direction for size fraction i, m.
κ constant in the lee sorting function.
λ bed form length, m.
λ_a bed form length averaged over a series of bed forms, m.
λ_b porosity.
Λ_i step length of size fraction i, m.
ν angle of repose, deg.
ρ density of water, kg m^{-3}.
ρ_s density of sediment, kg m^{-3}.
σ_a arithmetic standard deviation of the composition of the lee deposit; since its unit equals ϕ's unit, which is nonsensical (^{2}log mm), it is left out.
$\bar{\tau}_b$ bed shear stress averaged over a series of bed forms, N m^{-2}.
ϕ_i grain size of size fraction i on ϕ scale; since ϕ's unit is nonsensical (^{2}log mm), it is left out.
$\phi_{m\text{lee}}$ geometric mean grain size on ϕ scale of the lee deposit.
ω_i lee sorting function, specifying to what extent a specific size fraction that is transported over the bed form crest is deposited at elevation z of the lee face.

[56] **Acknowledgments.** The first author worked on the project in the pursuit of a doctoral degree at the Department of Civil Engineering of the University of Twente. The study was supported by the Institute for Inland Water Management and Waste Water Treatment (Rijkswaterstaat RIZA) of the Ministry of Transport, Public Works, and Water Management in the Netherlands, by WL Delft Hydraulics, and by the University of Twente. The Netherlands Organization for Scientific Research (NWO) and the Prince Bernhard Cultural Foundation are acknowledged for their financial support for a 3 month stay by the first author at the St. Anthony Falls Laboratory. Jan S. Ribberink and Huib J. de Vriend are gratefully acknowledged for their scientific support during the project.

References

Allen, J. R. L. (1965), Sedimentation to the lee of small underwater sand waves: An experimental study, *J. Geol.*, *73*, 95–116.
Armanini, A. (1995), Non-uniform sediment transport: Dynamics of the active layer, *J. Hydraul. Res.*, *33*, 611–622.
Armanini, A., and G. Di Silvio (1988), A one-dimensional model for the transport of a sediment mixture in non-equilibrium conditions, *J. Hydraul. Res.*, *26*, 275–292.
Bagnold, R. A. (1941), *The Physics of Blown Sand and Desert Dunes*, Methuen, New York.
Blom, A. (2003), A vertical sorting model for rivers with non-uniform sediment and dunes, Ph.D. thesis, Univ. of Twente, Enschede, Netherlands.
Blom, A., J. S. Ribberink, and H. J. de Vriend (2003), Vertical sorting in bed forms: Flume experiments with a natural and a trimodal sediment mixture, *Water Resour. Res.*, *39*(2), 1025, doi:10.1029/2001WR001088.
Crickmore, M. J., and G. H. Lean (1962), The measurement of sand transport by means of radioactive tracers, *Proc. R. Soc. London, Ser. A*, *266*, 402–421.
Di Silvio, G. (1992), Sediment exchange between stream and bottom: A four layer model, paper presented at the International Grain Sorting Seminar, Int. Assoc. for Hydraul. Res., Monte Verità, Ascona, Switzerland.
Einstein, H. A. (1937), Der Geschiebetrieb als Wahrscheinlichkeitsproblem, in *Mitteilung der Versuchsanstalt für Wasserbau an der Eidgenössische Technische Hochschule Zürich*, Verlag Rascher, Zurich, Switzerland. (English translation, *Sedimentation*, edited by H. W. Shen, pp. C1–C105, Fort Collins, Colo.)
Einstein, H. A. (1950), The bed-load function for sediment transportation in open channel flows, *Tech. Rep. 1026*, U.S. Dep. Agric. Soil Conserv. Serv., Washington, D. C.
Fernandez-Luque, R., and R. Van Beek (1976), Erosion and transport of bed-load sediment, *J. Hydraul. Res.*, *14*, 127–144.
Hirano, M. (1971), River bed degradation with armouring, *Trans. Jpn. Soc. Civ. Eng.*, *3*, 194–195.
Hirano, M. (1972), Studies on variation and equilibrium state of a river bed composed of nonuniform material, *Trans. Jpn. Soc. Civ. Eng.*, *4*, 128–129.
Hoey, T. B., and R. I. Ferguson (1994), Numerical simulation of downstream fining by selective transport in gravel bed rivers: Model development and illustration, *Water Resour. Res.*, *30*, 2251–2260.
Holly, F. M., Jr., and J. L. Rahuel (1990), New numerical/physical framework for mobile-bed modelling, part I—Numerical and physical principles, *J. Hydraul. Res.*, *28*, 401–416.
Kleinhans, M. G. (2002), Sorting out sand and gravel: Sediment transport and deposition in sand-gravel bed rivers, Ph.D. thesis, Utrecht Univ., Netherlands.
Kleinhans, M. G. (2004), Sorting in grain flows at the lee-side of dunes, *Earth Sci. Rev.*, *65*, 75–102, doi:10.1016/S0012-8252(03)00081-3.
McLean, S. R., J. M. Nelson, and S. R. Wolfe (1994), Turbulence structure over two-dimensional bed forms: Implications for sediment transport, *J. Geophys. Res.*, *99*, 12,729–12,747.
Nakagawa, H., and T. Tsujimoto (1980), Sand bed instability due to bed load motion, *J. Hydraul. Div.*, *106*, 2029–2051.
Parker, G. (1991), Selective sorting and abrasion of river gravel. I. Theory, *J. Hydraul. Eng.*, *117*, 113–149.
Parker, G., C. Paola, and S. Leclair (2000), Probabilistic Exner sediment continuity equation for mixtures with no active layer, *J. Hydraul. Eng.*, *126*, 818–826.
Ribberink, J. S. (1987), Mathematical modelling of one-dimensional morphological changes in rivers with non-uniform sediment, Ph.D. thesis, Delft Univ. of Technol., Netherlands.
Sloff, C. J., H. R. A. Jagers, Y. Kitamura, and P. Kitamura (2001), 2D morphodynamic modelling with graded sediment, paper presented at the 2nd Symposium on River, Coastal and Estuarine Morphodynamics, Int. Assoc. for Hydraul. Res., Obihiro, Japan.
Toro-Escobar, C. M., G. Parker, and C. Paola (1996), Transfer function for the deposition of poorly sorted gravel in response to streambed aggradation, *J. Hydraul. Res.*, *34*, 35–53.
Tsujimoto, T. (1990), Instability of longitudinal distribution of fluvial bed-surface composition, *J. Hydrosci. Hydraul. Eng.*, *7*, 69–80.
Tsujimoto, T., and K. Motohashi (1990), Static armoring and dynamic pavement, *J. Hydrosci. Hydraul. Eng.*, *8*, 55–67.
Van Ledden, M., and Z. B. Wang (2001), Sand-mud morphodynamics in an estuary, paper presented at the 2nd Symposium on River, Coastal and Estuarine Morphodynamics, Int. Assoc. for Hydraul. Res., Obihiro, Japan.
Yalin, M. S. (1977), *Mechanics of Sediment Transport*, Pergamon, New York.

A. Blom, Water Engineering and Management, Civil Engineering, University of Twente, P.O. Box 217, 7500 AE Enschede, Netherlands. (a.blom@utwente.nl)
G. Parker, St. Anthony Falls Laboratory, University of Minnesota, Mississippi River at 3rd Avenue, Minneapolis, MN 55414, USA. (parke002@umn.edu)